doi:10.36487/ACG_repo/2435_D-20
9th International Conference and Exhibition on Mass Mining, Kiruna Sweden 17-19 September 2024

Impact of tightly spaced hydraulic fractures on cave behavior

T. Garza-Cruz[a], M. Fuenzalida[a] and C. Orrego[b]
[a]*Itasca Consulting Group, Inc., USA*
[b]*Newmont Corporation, Australia*

ABSTRACT

As cave mines exploit deeper orebodies, a better understanding of the effect pre-conditioning of the rock mass has on overall cave behavior becomes crucial to ensure caveability and promote a manageable air gap size. Pre-conditioning in the form of hydraulic fracturing has been successfully used at Cadia East Mine for the PC1 and PC2 panels. In this study, caving behavior for different footprint sizes was evaluated using numerical models with hydraulic fractures explicitly represented as discontinuity planes, and the results were compared to analogous cases without preconditioning. The ultimate goal was to better understand the effect the presence of preconditioning has on cave behavior and to identify the size of a panel that would not only ensure continuous caving for the vertical distance needed, but also results in a manageable air gap size under the conditions of a potential panel cave that would exist at an approximate depth of 1700 m, about 300 m below the current PC2 horizon. The analysis elucidated that preconditioning plays a role not only in the cave back propagation rate, but also on cave shape and, ultimately, overall recovery.

1 INTRODUCTION

As mines exploit deeper orebodies with increasingly competent and massive rock masses, preconditioning the orebody may become necessary to effectively initiate and propagate a cave while maintaining an acceptable air gap.

Cadia East mine, located in New South Wales, is one of Australia's largest gold mining operations. The establishment of Panel Cave 1 (PC1) at Cadia East commenced in early 2011 with its extraction level set at a depth of 1,200 m below the surface. Official production from PC1 began in 2013. Currently, ore is extracted from PC1 and its neighboring panel (PC2) with an extraction level at 1,400 m depth. Plans to further develop panel caves for the Cadia East deposit are underway as extensions to the current PC1 and PC2 operations occur to the West (PC2-3) and East (PC1-2/PC1-3) caves, as shown in Figure 1.

Hydraulic fracturing as a means to precondition the orebody has been successfully used at Cadia East Mine. This paper describes the result of a study aimed at understanding how the presence of tightly spaced hydraulic fractures would influence the behavior of a potential panel cave below the PC2 horizon that would exist at an approximate depth of 1700 m, about 300 m below the current PC2 horizon, as shown in Figure 1.

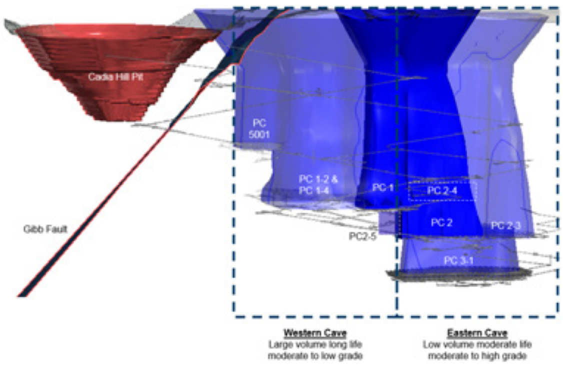

Figure 1 Location of panel caves at Cadia East.

2 NUMERICAL METHOD FOR ANALYSIS OF CAVING

A mine-scale *FLAC3D-MassFlow* hybrid model was constructed for caving analysis at Cadia East Mine. This approach can explicitly simulate the air gap formation and more complex mechanisms such as rilling within the mobilized zone and, therefore, is able to provide a more reliable prediction of caveability, cave propagation, and timing of breakthrough. In addition, the model can provide insights on the effect of cave-induced stresses and rock mass deformation on the performance of underground infrastructure. The flow component of the coupled *FLAC3D-MassFlow* model can provide information regarding dilution and recovery as well as fragmentation and fines migration.

2.1 Modeling Approach

The hybrid *FLAC3D-MassFlow* approach simulates the caving process by explicitly modeling each isolated movement zone (IMZ) derived from *MassFlow* in *FLAC3D* to determine the yielded zone, cave back, and air gap associated with mass drawn as introduced by Fuenzalida et al. (2018) in the hybrid *FLAC3D-REBOP* approach. After one cycle of extraction, *MassFlow* reports the location of the movement zones and the presence of air (if present) to the continuum *FLAC3D* model (Figure 2). *FLAC3D* solves stresses associated with the presence of these zones and estimates the yielded zone surrounding the cave. *FLAC3D* then informs *MassFlow* which zones (initially inactive) could now be mobilized. The procedure is repeated until the draw schedule, used as an input in *MassFlow*, is completed.

Figure 2 Conceptual scheme of the hybrid *FLAC3D-MassFlow* approach (after Fuenzalida et al., 2018).

2.2 Constitutive Model

As introduced by Pierce (2013), a numerical model that represents the caving process must account for the progressive failure and disintegration of the rock mass from an intact/jointed elastic condition to a fully broken material (bulked). In this complex process, creation of the cave results in deformation and stress redistribution of the rock mass above the undercut, failure of the rock mass in advance of the cave with an associated progressive reduction in strength from peak to residual levels, and dilation, bulking, fragmentation, and mobilization of the cave material.

This overall process of loading the rock mass to its peak strength, followed by post-peak reduction in strength to some residual level with increasing strain, is often termed as a strain-softening process and is the result of strain-dependent material properties.

The Itasca Model for Advanced Strain Softening (*IMASS*) constitutive model (Ghazvinian et al., 2020) was used in this study. *IMASS* is a strain-softening model for the simulation of rock mass response to mining. This model contains a two-stage softening behavior as shown in Figure 3. The first residual envelope (blue line) represents the post-peak strength. At this point, the rock mass is assumed to have undergone fracturing, but the resulting rock fragments are still fully interlocked. The second residual envelope (green line) represents the ultimate residual strength at the point of maximum bulking. At this point, the degree of rock fragment interlock is at its minimum, and the porosity is maximized.

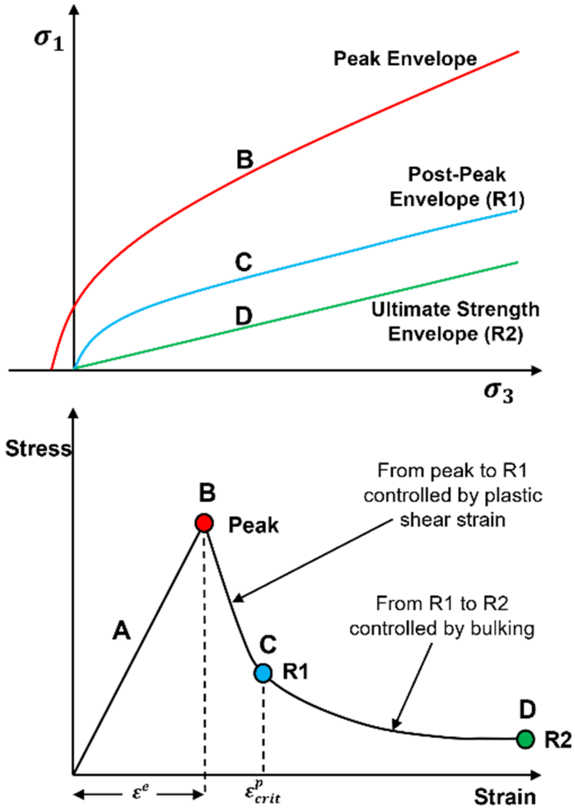

Figure 3 Yield surfaces and material response for *IMASS* model (after Ghazvinian et al., 2020).

3 GEOTECHNICAL CONSIDERATIONS

3.1 Rock Mass Properties

The rock mass strength properties listed in Table 1 were used in the present analysis. These properties resulted in a large-scale rock mass strength on the order of 30 MPa, which is considered to be on the conservative side for the area of interest (300 m below PC2 horizon) but deemed appropriate given the current level of uncertainty.

Table 1 Rock Mass Properties Used for the Volcanic Unit at Cadia

σ_{ci}	120 MPa
GSI	75
mi	24.5
Young's Modulus	29.8 GPa
Density	2970 kg/m^3

The presence of preconditioning in the form of hydraulic fractures (HFs) with 4 m spacing and dipping 5° was explicitly represented as planar discontinuities with zero cohesion, zero tensile strength, and a friction angle of 45°.

3.2 In-Situ Stress

The in-situ stress magnitudes and orientations listed in Table 2 were used in all models presented in this study. Although the present study focuses on the caving behavior below the PC2 horizon conditions, the influence of current mining (i.e., PC2 cave) on the stress state is not accounted for. This is a conservative assumption since the PC2 cave would have induced a redistribution of stresses below the cave that would aid caveability of a cave back propagating from below.

Table 2 Cadia East Stress Tensor Used

Principal Stress	Magnitude [Pa]	Orientation
σ_v	2970*9.81*depth	Vertical
σ_H	1.78* σ_v	E-W
σ_h	1.16* σ_v	N-S

4 THREE-DIMENSIONAL ANALYSIS OF THE EFFECT OF PRECONDITIONING ON CAVING

A full 3D model with explicit hydraulic fractures represented as discontinuity planes at 4 m spacing and dipping 5° was created (orthogonal to the minimum principal stress orientation). The undercut level and drawbells were explicitly represented and are shown in Figure 4.

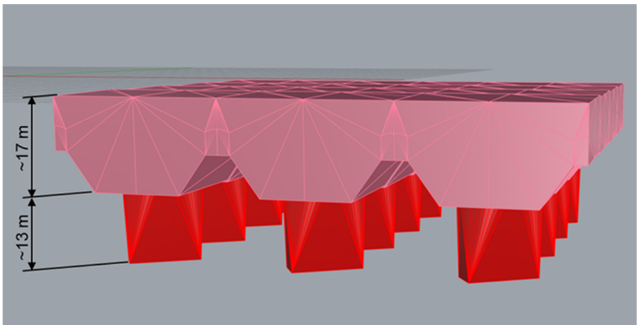

Figure 4 Drawbell and undercut geometry implemented in the 3D models.

Three footprints with hydraulic radii (HR) of 15, 21, and 31 m were evaluated using the development sequence and production schedule shown in Figure 5.

Footprints with hydraulic radii of 15 m and 21 m were initially evaluated in the context of cave establishment as shown in Figure 6 and Figure 7, respectively.

The results indicate that for the same geomechanical conditions, increasing the HR and keeping the analogous draw rate per drawpoint increases the vertical cave growth, which in turn decreases the airgap size. The presence of preconditioning contributes to a flatter cave back, aiding caveability compared to a cave that develops a more tapered geometry.

Overall, the case with HR of 15 m developed an air gap size comparable to the height of the muck pile as caving was initiated. Ultimately, the size of an acceptable air gap depends on the risk tolerance of each mine. For the case of Cadia East, an air gap on the order of <10 m was considered in the acceptable range (personal communication, Cristian Orrego, 2023). Therefore, although caving was initiated for the case with HR of 15 m, the large air gap size makes it an undesirable case.

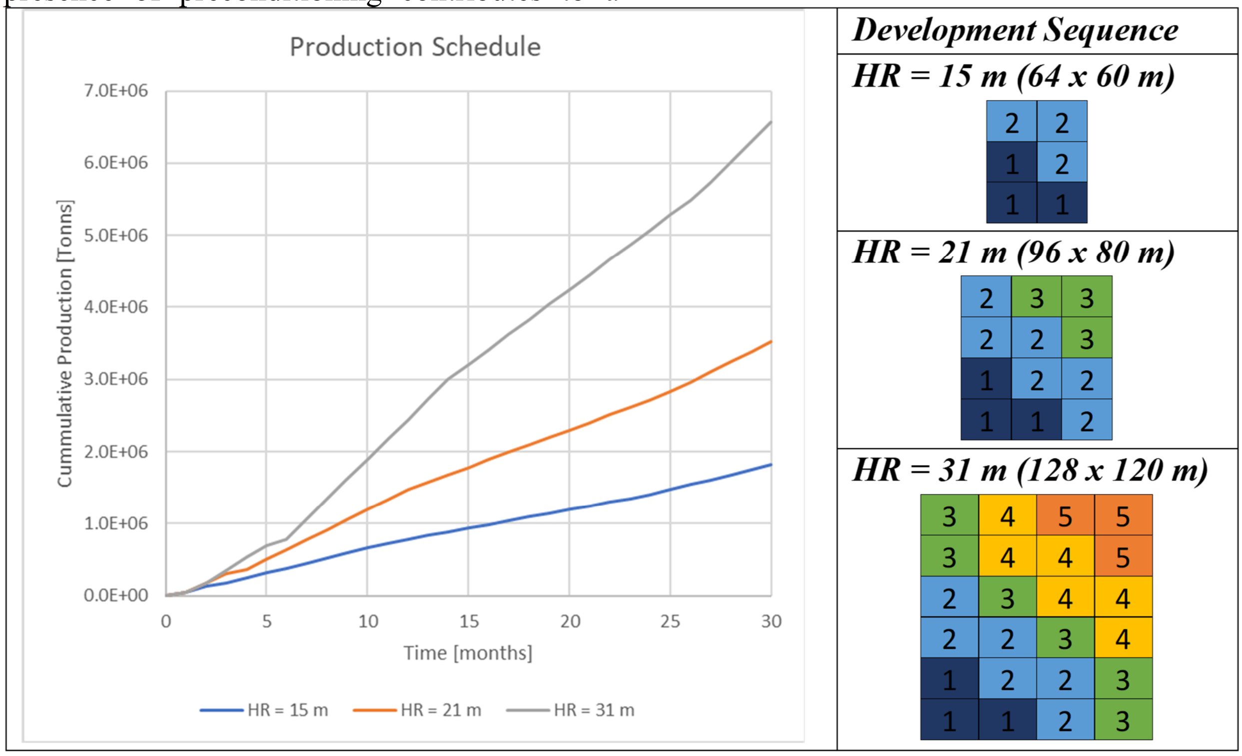

Figure 5 Production schedule and development sequence for the three footprints analyzed.

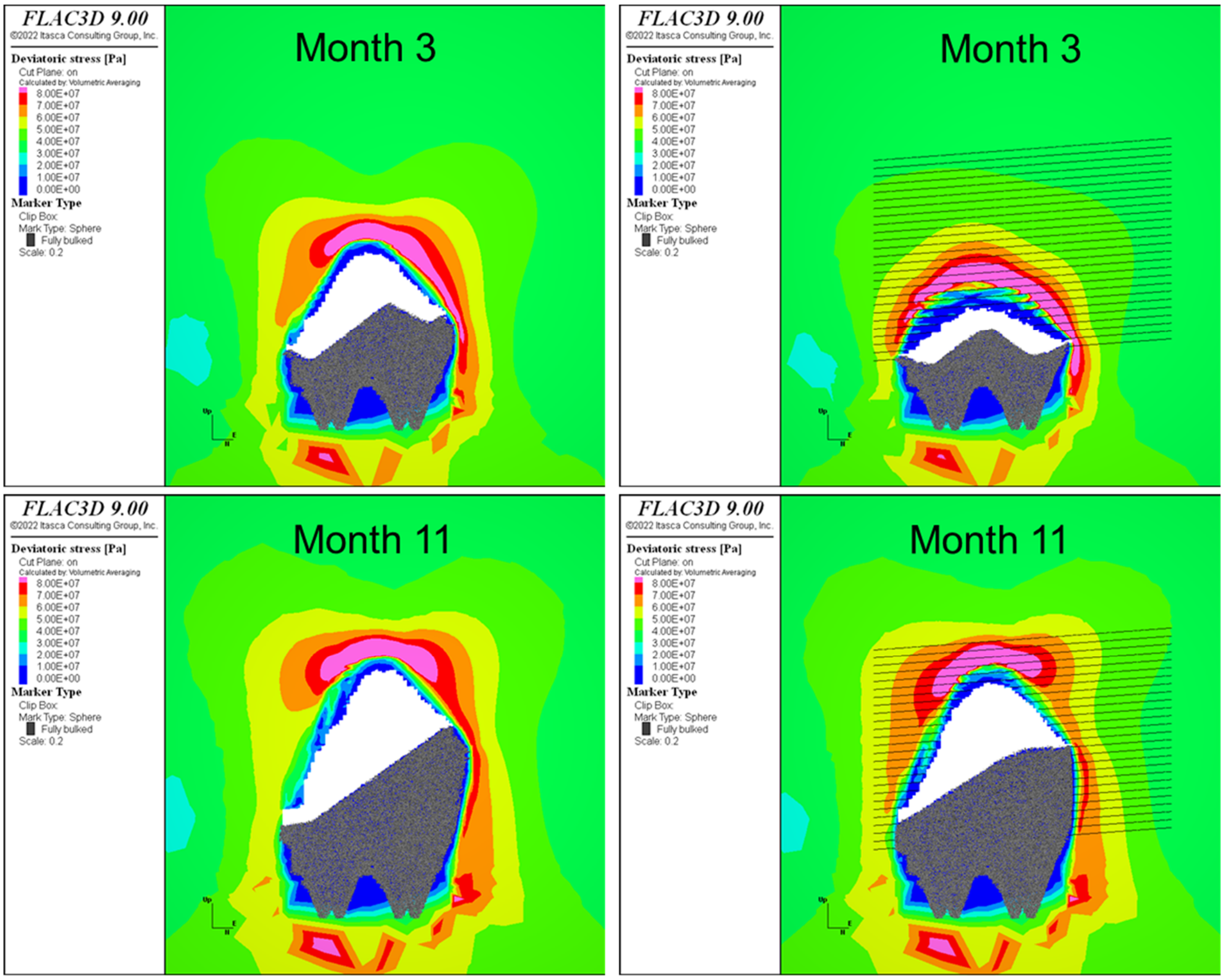

Figure 6 **Cave establishment at 1700 m depth for the case of HR = 15 m without and with preconditioning (left and right, respectively).**

Given the draw schedule described in Figure 5, the caves propagated from two footprint HRs (21 m and 31 m) were evaluated over a 300-m high column, representing the approximate column height that a potential panel cave below the PC2 horizon would need to propagate to reach the PC2 level. The ultimate goal of this analysis was to better understand the effect of the presence of preconditioning on cave behavior and to identify the size of a panel that would not only ensure continuous caving for the distance needed, but also results in a manageable air gap size under the studied conditions while minimizing potential loss/sterilization of ore.

Figure 8 shows the deviatoric stresses resulting from cave propagation of approximately 150 m and 300 m for the case with HR of 21 m. Figure 9 shows different isometric views of the fracture zone, mobilized zone, and air gap as a result of caving halfway and through the full 300 m column. In general, preconditioning contributes to a flatter cave back, aiding caveability and significantly improving recovery, compared to a cave that develops a more tapered geometry. The effect preconditioning has on recovery is especially noticeable when comparing the north views of the full cave in Figure 9. The presence of HFs tends to widen the cave (even beyond the footprint size) and contribute towards a cave shape that engulfs more of the volume above the footprint projection, promoting higher recovery. In contrast, the case with no preconditioning develops a more tapered cave shape, potentially sterilizing a volume of the ore. The effect the presence of preconditioning has on the average height of material mobilized and available for recovery (calculated as the total mobilized volume divided by the footprint area) can be seen in graphical form in Figure 10, resulting in approximately 47% more caved rock mobilized for the preconditioned case. The results elucidated that the presence of preconditioning in the form of HFs reduces the brittleness of the rock mass (HFs can accommodate some shear strain), while the flatter shape of the cave back with HFs also leads to the induced stresses acting on a larger volume of rock, compared to a smaller and more targeted volume of rock where induced stresses concentrate when a more tapered cave back shape is present (virgin case), which delays the cave back propagation to reach the 300 m mark. Once the cave back reaches the PC2 horizon, dilution will be free to enter the column; therefore, maximizing recovery before this stage is highly desirable and more achievable with preconditioning.

It is important to recognize that the shape of the cave is sensitive to the draw schedule, which is more pronounced during cave establishment. A draw schedule should be carefully designed and paired with draw control to make the cave as symmetrical as possible to promote maximization of recovery.

Figure 11 shows the air gap development as a function of production for the case with hydraulic radius of 21 m. For reference, the dotted gray line denotes an air volume equivalent to the footprint of the cave multiplied by a height of 10 m. The observed increases and decreases in air gap size are directly related to the change in the production rate simulated (see Figure 5), with higher production rates leading to larger air gaps. The results elucidated that the presence of hydraulic fractures reduces the air gap size compared to the virgin case, lowering the air blast risk. If a smaller air gap for the case with HR of 21 m is desired, production would need to take place at a lower rate.

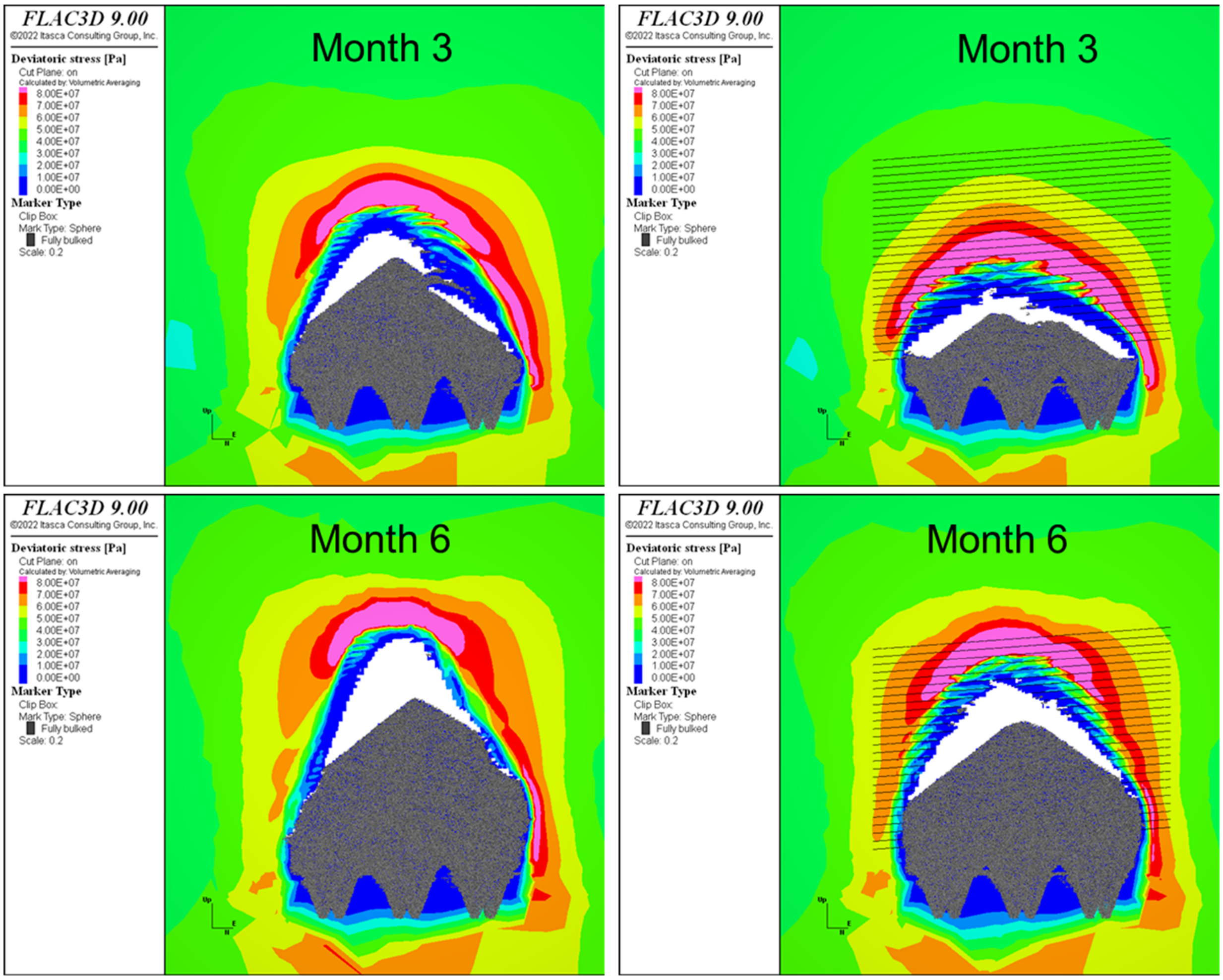

Figure 7 **Cave establishment at 1700 m depth for the case of HR = 21 m without and with preconditioning (left and right, respectively).**

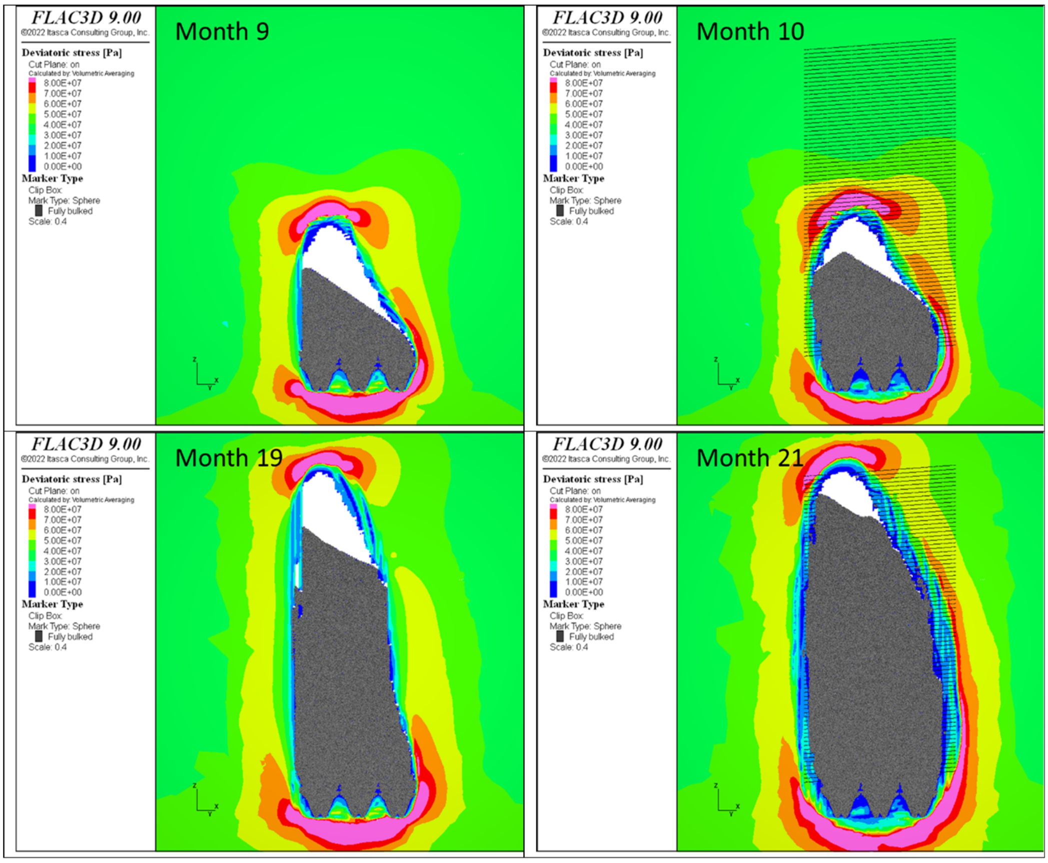

Figure 8 **Deviatoric stresses at 1700 m depth for the case of HR = 21 m at approximately 150 m (top) and 300 m (bottom) cave height without and with preconditioning (left and right, respectively).**

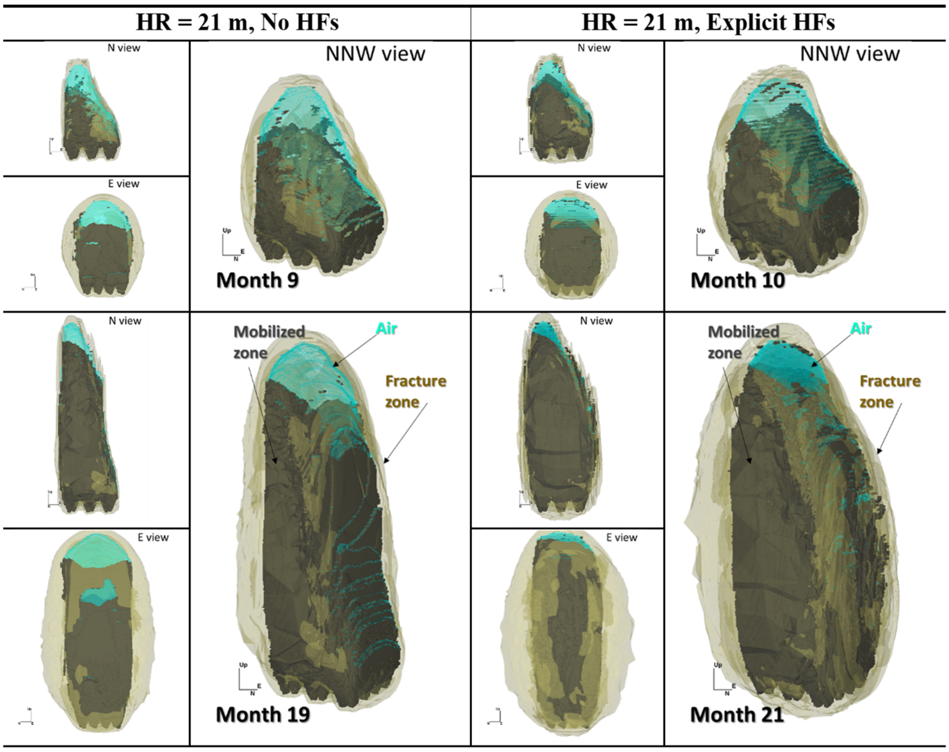

Figure 9 **Cave shape at 1700 m depth for the case of HR = 21 m at approximately 150 m (top) and 300 m (bottom) height without and with preconditioning (left and right, respectively).**

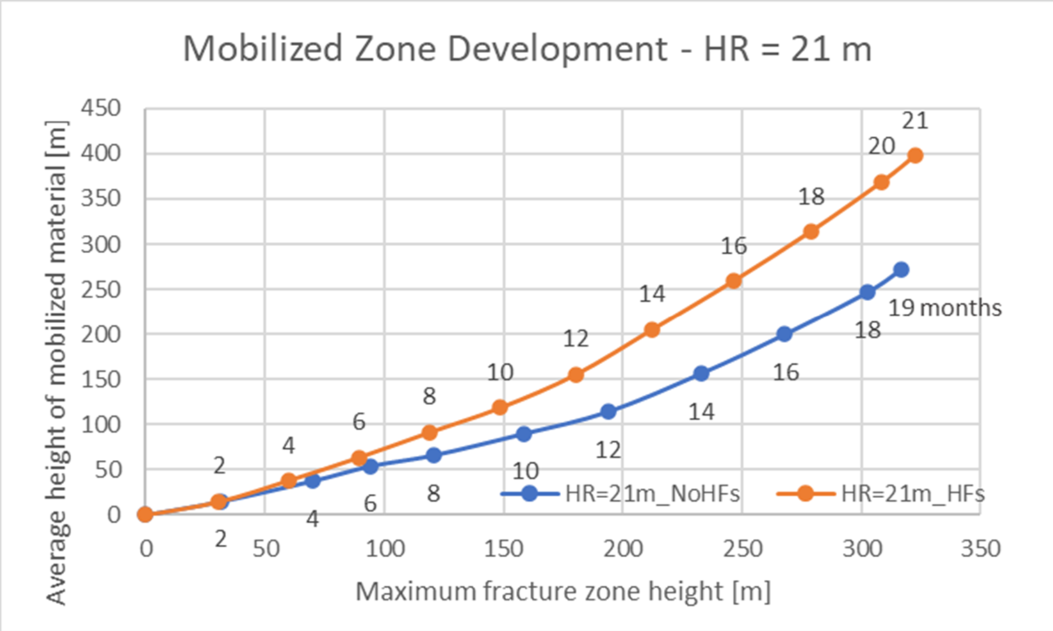

Figure 10 Mobilized zone development as a function of fracture zone height for the case with hydraulic radius of 21 m. This is the caved material available for recovery.

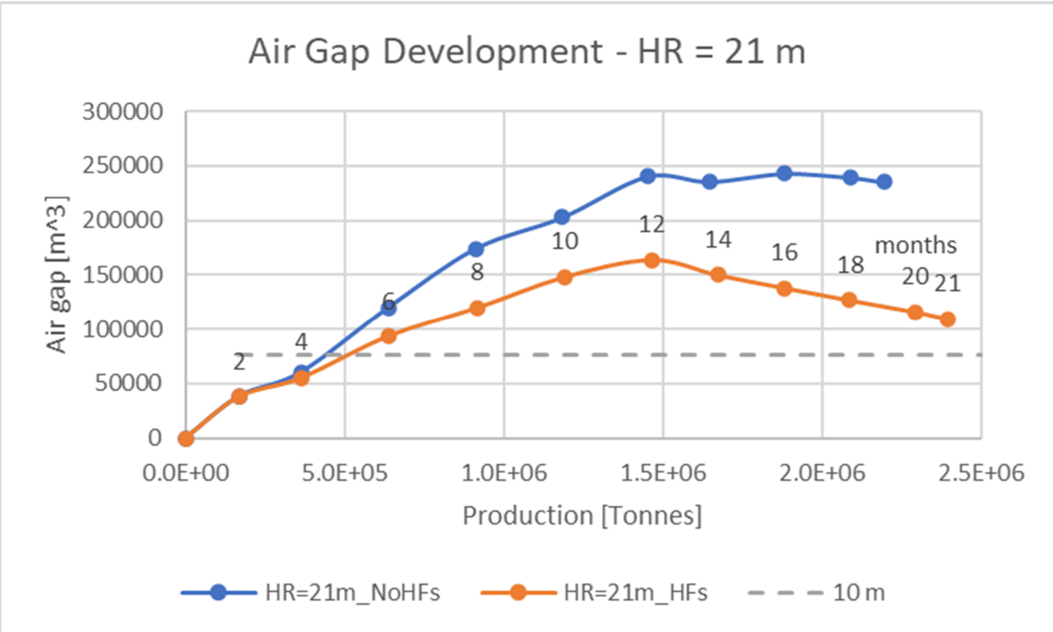

Figure 11 Air gap development as a function of production for the case with hydraulic radius of 21 m. The gray dotted line denotes an air volume 10 m high.

Figure 12 and Figure 13 show the deviatoric stresses and different isometric views of the cave, respectively, with HR of 31 m when the cave has reached a height of approximately 150 m and 300 m. Similar to what was observed in the case with HR of 21 m, the presence of hydraulic fractures contributes to a flatter cave back that widens the cave (even beyond the footprint size), mobilizing a larger volume of rock, improving recovery. The effect preconditioning has on recovery is especially noticeable when comparing the north views of the full cave in Figure 13. The effect the presence of preconditioning has on the average height of material mobilized and available for recovery (calculated as the total mobilized volume divided by the footprint area) can be seen in graphical form in Figure 14, resulting in approximately 31% more caved rock mobilized for the preconditioned case with HR of 31 m compared to the virgin case. As previously observed, the presence of preconditioning in the form of HFs reduces the brittleness of the rock mass (HFs can accommodate some shear strain), while the flatter shape of the cave back with HFs also leads to the induced stresses acting on a larger volume of rock, compared to a smaller and more targeted volume of rock where induced stresses concentrate when a more tapered cave back shape is present (virgin case), which delays the cave back propagation reaching the 300 m mark (PC2 horizon). Therefore, preconditioning allows for maximizing recovery through caving a larger volume of rock before the cave back reaches the PC2 horizon and dilution is free to enter the column.

Figure 15 shows the air gap development as a function of the production schedule used (Figure 5) for the case with hydraulic radius of 31 m. For reference, the dotted gray line denotes an air volume equivalent to the footprint of the cave multiplied by a height of 10 m. As previously noted, the observed increases and decreases in air gap size are directly related to the change in the production rate simulated, with higher production rates leading to larger air gaps. The results confirmed that the presence of hydraulic fractures reduces the air gap size compared to the virgin case, which lowers the air blast risk. Additionally, for the production schedules used (Figure 5), by increasing the footprint HR from 21 m to 31 m, the size of the associated air gap is significantly reduced to be well below the 10 m mark. This provides an opportunity for exploring a more aggressive production schedule (while keeping the air gap just below 10 m) for the case with HR of 31 m.

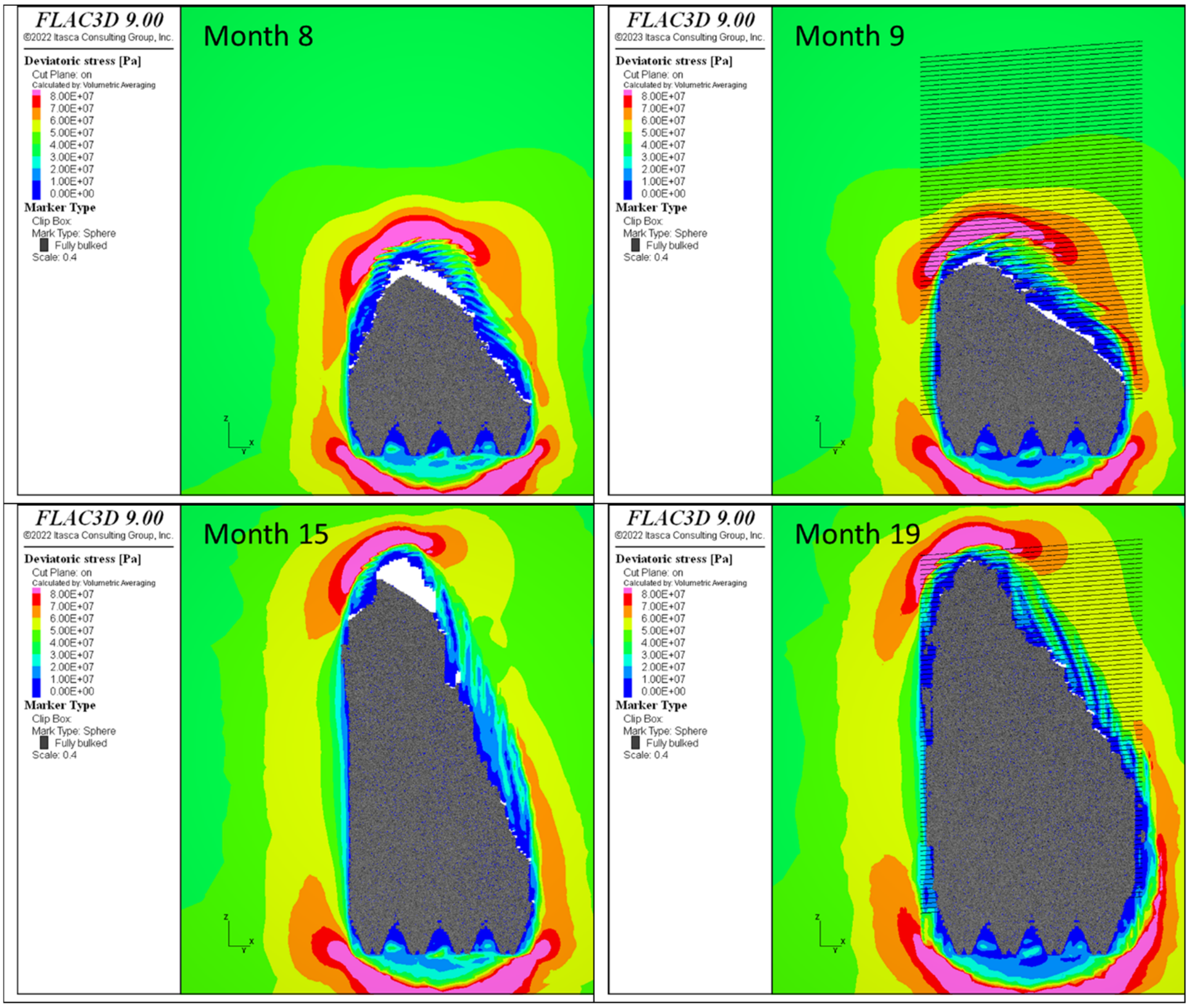

Figure 12 Deviatoric stresses at 1700 m depth for the case of HR = 31 m at approximately 150 m (top) and 300 m (bottom) cave height without and with preconditioning (left and right, respectively).

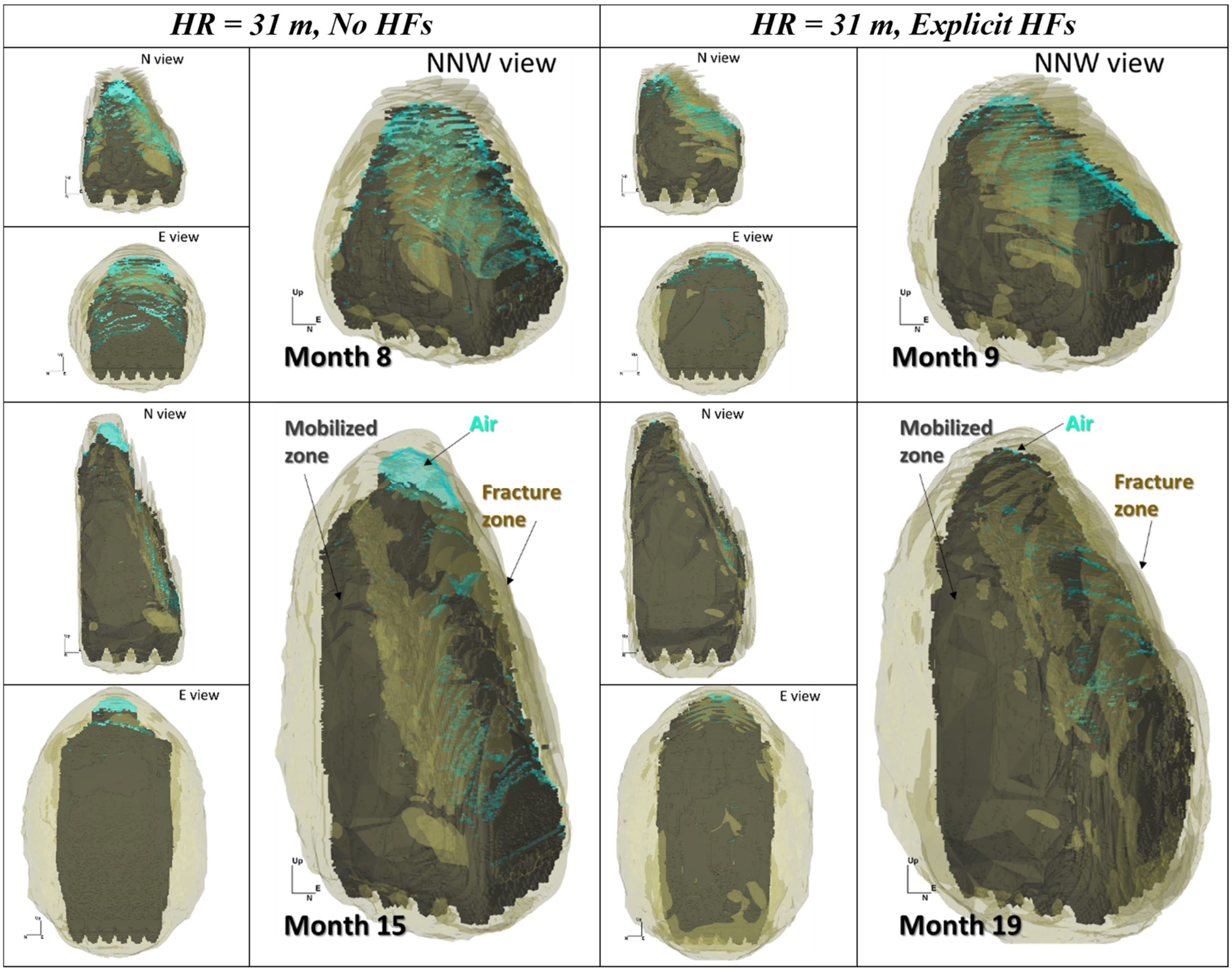

Figure 13 Cave shape at 1700 m depth for the case of HR = 31 m at approximately 150 m (top) and 300 m (bottom) height without and with preconditioning (left and right, respectively).

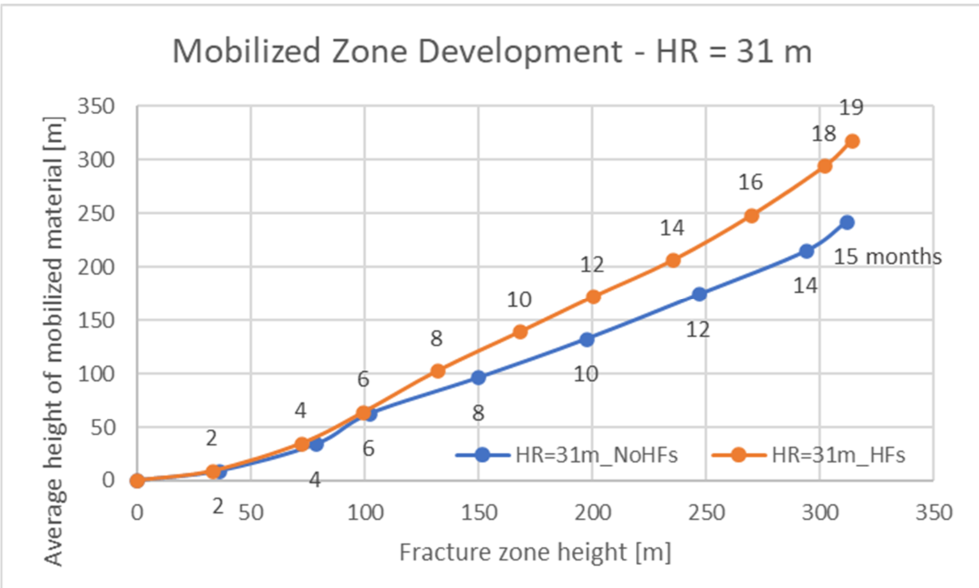

Figure 14 Mobilized zone development as a function of fracture zone height for the case with hydraulic radius of 31 m. This is the caved material available for recovery.

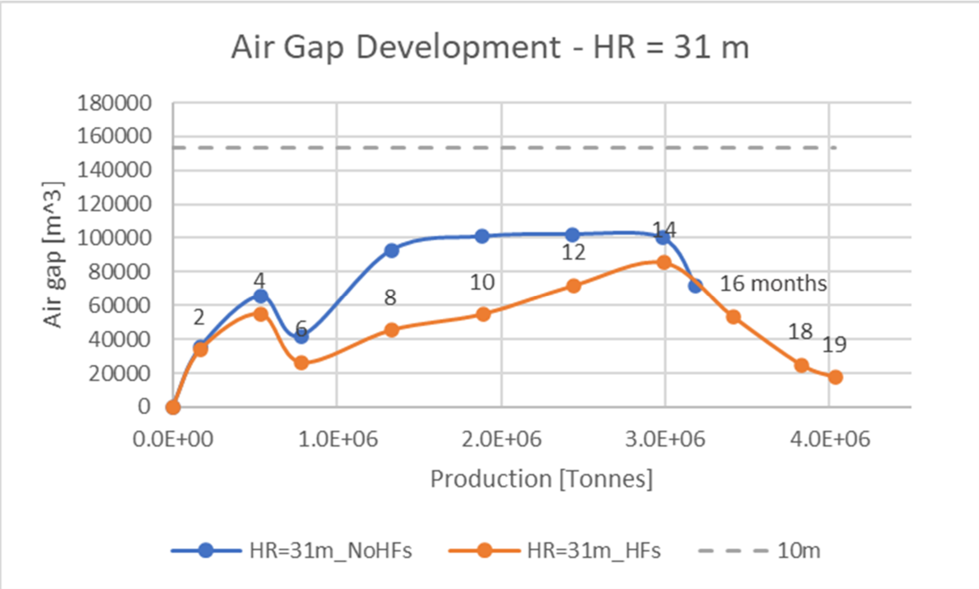

Figure 15 Air gap development as a function of production for the case with hydraulic radius of 31 m. The gray dotted line denotes an air volume 10 m high.

5 CONCLUSIONS

The ultimate goal of this analysis is to better understand the effect of the presence of preconditioning on cave behavior and to identify the size of a panel that would not only ensure continuous caving for the distance needed, but that also results in a manageable air gap size under the studied conditions (1700 m depth).

The results of this work elucidated that the presence of hydraulic fractures contributes to a flatter cave back, which aids caveability and is able to mobilize a larger volume of rock, significantly improving recovery compared to a cave that develops a more tapered geometry under virgin conditions. The presence of preconditioning in the form of HFs reduces the brittleness of the rock mass (HFs can accommodate some shear strain), while the flatter shape of the cave back with HFs also leads to the induced stresses acting on a larger volume of rock, compared to a smaller and more targeted volume of rock where induced stresses concentrate when a more tapered cave back shape is present (virgin case), which delays the cave back propagation reaching the 300 m mark (PC2 horizon). Therefore, preconditioning allows for maximizing recovery through caving of a larger volume of rock before the cave back reaches the PC2 horizon and dilution is free to enter the column. Additionally, the presence of hydraulic fractures reduces the air gap size, resulting in lower air blast risk.

In general, increasing the hydraulic radius of the cave footprint allows the cave back to propagate faster and reduces the air gap size. Under the conditions studied, a hydraulic radius of 31 m kept the air gap well below the 10 m mark; therefore, an opportunity could exist for a more aggressive production schedule.

It is important to keep in mind that under equivalent geomechanical conditions, the air gap size is a function of both cave propagation and production rate. The shape of the cave is sensitive to the draw schedule, especially during cave establishment. Therefore, a draw schedule should be carefully designed and paired with draw control to make the cave as symmetrical as possible to maximize recovery.

6 LIMITATIONS AND FUTURE WORK

In this study, hydraulic fractures are represented as planar discontinuities with an apparent friction angle of 45°. In reality, the hydraulic fractures resulting from a preconditioning program would not be planar and would have a roughness associated to them. The effect these geometrical and physical characteristics have on the resulting cave propagation rate and associated air gap size should be evaluated.

REFERENCES

Fuenzalida, M., Pierce, M. & Katsaga, T. (2018). REBOP-FLAC3D hybrid approach to cave modelling, in Proceedings of the Fourth International Symposium on Block and Sublevel Caving (Vancouver, Canada 2018), Y Potvin & J Jakubec (eds), pp. 297-312. Perth: Australian Centre for Geomechanics.

Ghazvinian, E., Garza-Cruz, T., Bouzeran, L., Fuenzalida, M., Cheng, Z., Cancino, C. & Pierce, M. (2020). Theory and Implementation of the Itasca Constitutive Model for Advanced Strain Softening (IMASS), 8th International Conference & Exhibition on Mass Mining, MassMin 2020, 451–461. Santiago: University of Chile.

Itasca Consulting Group, Inc. (2023a). FLAC3D — Fast Lagrangian Analysis of Continua in Three Dimensions (Version 9.0). Minneapolis: Itasca.

Itasca Consulting Group, Inc. (2023b). MassFlow — A gravity flow simulator (Version 9.0). Minneapolis: Itasca.

Pierce, M. E. (2013). Numerical Modeling of Rock Mass Weakening, Bulking and Softening Associated with Cave Mining. ARMA e-Newsletter Spring 2013, 9.